



Effect of Fe/SiO₂ and CaO/SiO₂ mass ratios on metal recovery rate and metal content in slag in oxygen-enriched direct smelting of jamesonite concentrate

Zhong-tang ZHANG, Xi DAI

School of Metallurgical and Environment, Central South University, Changsha 410083, China

Received 20 April 2019; accepted 4 December 2019

Abstract: The oxygen-enriched direct smelting of jamesonite concentrate was carried out at 1250 °C by changing the slag composition. The effects of Fe/SiO₂ and CaO/SiO₂ mass ratios on the metal recovery rate as well as metal content in slag were investigated. Experimental results indicated that the metal (Pb+Sb) recovery rate was up to 88.30%, and metal (Pb+Sb) content in slag was below 1 wt.% under the condition of slag composition of 21–22 wt.% Fe, 19–20 wt.% SiO₂ and 17–18 wt.% CaO with Fe/SiO₂ mass ratio of 1.1:1 and CaO/SiO₂ mass ratio of 0.9:1. The microanalysis of the alloy and slag demonstrated that the main phases in the alloy contained metallic Pb, metallic Sb and a small amount of Cu₂Sb and FeSb₂ intermetallic compounds. The slag was mainly composed of kirschsteinite and fayalite. Zinc in the raw material was mainly oxidized into the slag phase in the form of zinc oxide.

Key words: jamesonite concentrate; metallurgical process intensification; slag type; pyrometallurgy; oxygen-enriched direct smelting

1 Introduction

Lead and antimony are considered to be very important metals due to their wide applications in fire retardants, storage batteries, metallurgy and radiation protection [1]. Jamesonite concentrate is a complex sulfide ore, which has become one of important raw materials for the production of lead and antimony in China [2]. The traditional routes for lead and antimony extraction from jamesonite concentrate include fluidized-bed roasting, sintering, blast furnace reduction, reverberatory furnace converting and refining. Nevertheless, the process causes serious problems such as long process flow, low concentration SO₂ emissions, high energy consumption and low metal recovery rate [3]. At present, oxygen-enriched direct smelting of lead/copper sulfide ore has been widely adopted in

industry, which has greatly shortened the process flow and solved the problem of low concentration of sulfur dioxide pollution [4,5]. Whether the oxygen-enriched direct smelting process could be carried out smoothly with ideal technical and economic indicators, to a certain extent, depends on the slag type [6]. The mass ratios of Fe/SiO₂ ($m(\text{Fe})/m(\text{SiO}_2)$) and CaO/SiO₂ ($m(\text{CaO})/m(\text{SiO}_2)$) are very important parameters during smelting, which could affect the metal recovery rate and metal content in slag. FU [7] proposed that the slag with high content of CaO could improve the output of crude lead during smelting. Meanwhile, the lead content in slag could be reduced to 1.47%. YANG [8] found that the slag with medium content of SiO₂ and low content of Fe_xO_y was beneficial to the QSL lead smelting process when the iron content in the concentrate was approximately 5%. However, selecting the slag with medium contents

of SiO_2 and Fe_xO_y or medium content of SiO_2 and high content of Fe_xO_y was beneficial to the smelting process when the iron content in the concentrate was beyond 8%. ZHOU [9] investigated the slag type in oxygen-enriched bath smelting of stibnite concentrate, and found that the reasonable slag type was $m(\text{Fe})/m(\text{SiO}_2)$ 0.7:1 and $m(\text{CaO})/m(\text{SiO}_2)$ 0.5:1. The antimony content in slag was as low as 0.37%. Based on the above ideas, a novel technology of the oxygen-enriched direct smelting of jamesonite concentrate to obtain the lead–antimony alloy has been proposed by our group [10–12]. However, in previous study, the thermodynamic analysis and reaction mechanism of the oxygen-enriched direct smelting of jamesonite concentrate have been investigated, but few studies about the effect of slag type on the smelting process have been reported [13,14].

In this study, the effects of $m(\text{Fe})/m(\text{SiO}_2)$ and $m(\text{CaO})/m(\text{SiO}_2)$ on the metal recovery rate and metal content in slag in oxygen-enriched direct smelting of jamesonite concentrate were investigated in the laboratory scale, and the microstructure and characteristics of the smelting products were identified.

2 Experimental

2.1 Materials

The jamesonite concentrate (JC) and antimony blast furnace slag (ABFS) were obtained from Jinchengjiang Smelter, Guangxi, China. The chemical composition analysis showed that the jamesonite concentrate used in this work mainly contained 21.94 wt.% Pb, 17.16 wt.% Sb, 9.88 wt.% Fe, 11.10 wt.% SiO_2 , 5.63 wt.% CaO and 15.50 wt.% S. The antimony blast furnace slag utilized in this work mainly contained 13.62 wt.% CaO, 24.94 wt.% Fe, 22.90 wt.% SiO_2 and 12.11 wt.% Zn. The phases of jamesonite, galena, sphalerite, pyrite, carbonate and quartz were identified in the jamesonite concentrate through optical microscope technique (Fig. 1). The XRD pattern of jamesonite concentrate is shown in Fig. 2. The peaks found at different diffraction angles were matched with $\text{FePb}_4\text{Sb}_6\text{S}_{14}$ (jamesonite, JCPDS, No. 42–1391), PbS (galena, JCPDS, No. 77–0244), FeS_2 (pyrite, JCPDS, No. 421340) and ZnS (sphalerite, JCPDS, No. 05-0566). Experimental flux used in this work contained analytically pure

ferric oxide (Fe_2O_3 , 69.8–70.1 wt.%, Xilong Scientific, Shantou, China), calcium oxide (CaO, 98.0 wt.%, Xilong Scientific, Shantou, China) and silicon dioxide (SiO_2 , 99.0 wt.%, Xilong Scientific, Shantou, China).

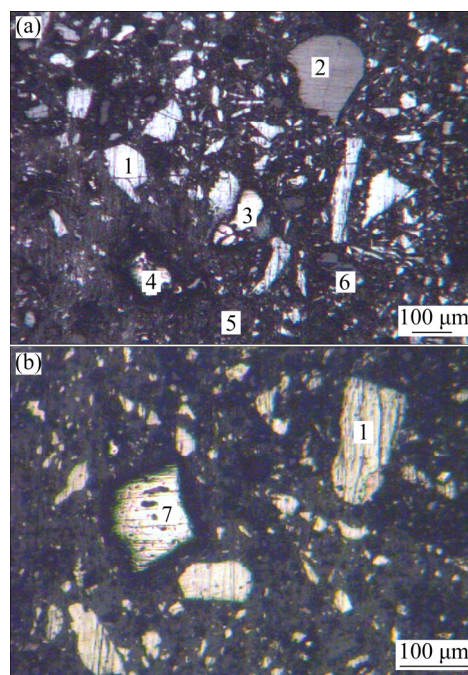


Fig. 1 Optical micrographs (in reflected light) of jamesonite concentrate: 1—Jamesonite; 2—Sphalerite; 3, 4—Pyrite; 5—Carbonate; 6—Quartz; 7—Galena

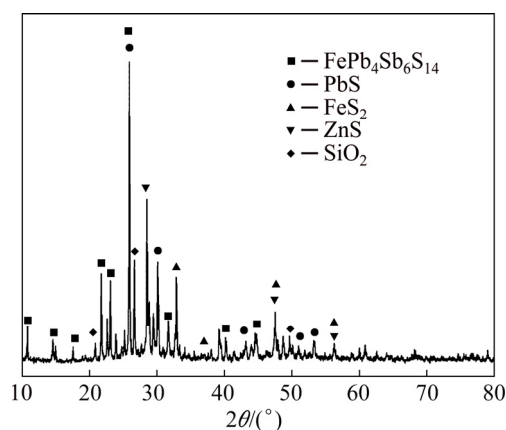


Fig. 2 XRD pattern of jamesonite concentrate

2.2 Experimental method

Experiments were carried out in a self-designed electric furnace. Furnace temperature was measured by using a calibrated Pt–Rh thermocouple. The temperature accuracy was estimated to be ± 2 K for the entire experimental temperature. The temperature data were collected

by using a temperature controller. The schematic diagram of experimental apparatus is shown in Fig. 3.

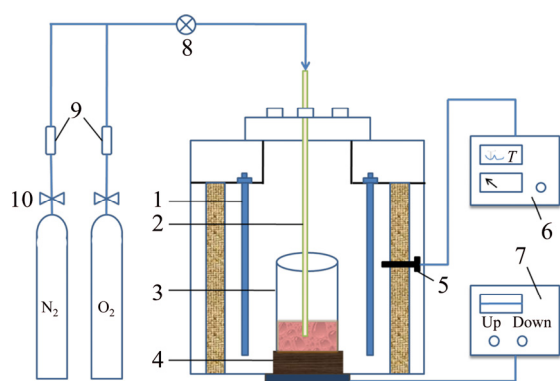


Fig. 3 Schematic diagram of experimental apparatus: 1—SiC heating elements; 2—Alundum tube; 3—Reaction vessel; 4— Fire-resistant pad; 5— Thermocouple; 6— Temperature controller; 7— Elevator controller; 8—Pressure valve; 9—Rotor flowmeter; 10—Swirling valve

For this, 300 g jamesonite concentrate and 2000 g pre-weighed antimony blast furnace slag and flux (the mass ratio of flux to antimony blast furnace slag is below 10%) were mixed homogeneously and added to the reaction vessel. When the furnace temperature was raised to the given temperature, the reaction vessel was placed into the electric furnace for a melting of 1 h first, then oxidation smelting with blowing oxygen-enriched gas. The experiments were carried out under the condition of 1250 °C for the smelting temperature, 60% for the oxygen concentration, 0.18 MPa for the gas pressure, 0.08 m³/h for the oxygen flow rate, 1 h for the reaction time, and 40 min for the clarification time. After that, the reaction vessel was taken out quickly and cooled down to the room temperature in air. Finally, the alloy and smelting slag were weighed and analyzed, respectively. The alloy recovery rate is calculated using the following equation:

$$R_A = \frac{m_{\text{alloy}} w(\text{Pb} + \text{Sb})_{\text{alloy}}}{m_{\text{JC}} w(\text{Pb} + \text{Sb})_{\text{JC}} + m_{\text{ABFS}} w(\text{Pb} + \text{Sb})_{\text{ABFS}}} \quad (1)$$

where R_A is the recovery rate of alloy; m_{JC} , m_{ABFS} and m_{alloy} are the masses of jamesonite concentrate, antimony blast furnace slag and alloy, respectively; $w(\text{Pb} + \text{Sb})_{\text{JC}}$, $w(\text{Pb} + \text{Sb})_{\text{ABFS}}$ and $w(\text{Pb} + \text{Sb})_{\text{alloy}}$ are the metal contents (Pb+Sb) in jamesonite concentrate, antimony blast furnace slag and alloy, respectively.

2.3 Analysis and testing

The metal contents in the alloy and slag of smelting process were analyzed through volumetric method. The crystal phase of the alloy and slag produced during smelting was determined by using X-ray diffraction analysis (Cu K α , $\lambda=0.154056$ nm; Rigaku-TTR III). The ore phase of jamesonite concentrate was identified through the optical microscope technique (OM, LEICA DMRX). The surface morphologies of the alloy and slag were determined by scanning electron microscopy (SEM, JSM-6360LV) and the elemental analysis by X-ray energy dispersive spectroscopy (EDS, EDX-GENESIS 60S).

3 Results and discussion

3.1 Slag type selection

The gangue composition of jamesonite concentrate was mainly composed of silicon dioxide and calcium oxide, which also contained about 10% iron. Therefore, FeO–SiO₂–CaO slag system was mainly adopted in the industrial production. The phase diagram of FeO–SiO₂–CaO ternary slag system is shown in Fig. 4 [15]. Previous research [16] illustrated that the ternary slag system was also suitable for the oxygen-enriched direct smelting of jamesonite concentrate, and the smelting temperature was approximately 1250 °C. Hence, the fusing temperature of the slag should not be higher than 1200 °C, where the red zone surrounded by 1200 °C isotherms. Combined with the actual production, the *ABCD* zone ($m(\text{Fe})/m(\text{SiO}_2)$ (1.0–1.4):1, $m(\text{CaO})/m(\text{SiO}_2)$ (0.6–1.0):1) in Fig. 4 was selected as the research scope of slag composition, where the *EFG* line represented 1200 °C isotherm and *HI* line represented 1250 °C isotherm. According to Fig. 4, the *AEFGD* shaded zone was located in the 1200 °C isothermal interior. That is, the fusing temperature of the slag in the shadow zone was below 1200 °C, which could be considered as the selected zone of slag composition in this study.

The viscosity of slag had a significant effect on the agitation strength of the molten bath and the separation of the slag and alloy in oxygen-enriched direct smelting of jamesonite concentrate, which would further affect the metal recovery rate and metal loss to slag. The viscosity of slag with composition points of 1–9 in Fig. 4 was calculated

by thermodynamic software Factsage [17], and the results are presented in Fig. 5. As can be seen in Fig. 5(a), it was discovered that the viscosity of slag was below 0.5 Pa·s at 1200 °C and 1250 °C under the condition of $m(\text{Fe})/m(\text{SiO}_2)$ 1.1:1 when $m(\text{CaO})/m(\text{SiO}_2)$ increased in the range of 0.6:1–0.8:1, which was beneficial to the smelting process. However, when $m(\text{CaO})/m(\text{SiO}_2)$ further increased to 0.9:1–1.0:1, the viscosity of slag was beyond 0.5 Pa·s at 1200 °C while below 0.5 Pa·s at 1250 °C, which indicated that the slag fluidity would be deteriorated at 1200 °C. From Fig. 5(b), it was observed that the viscosity of slag was higher than 0.5 Pa·s at 1200 °C while lower than 0.5 Pa·s at 1250 °C under the condition of $m(\text{CaO})/m(\text{SiO}_2)$ 0.9:1 when $m(\text{Fe})/m(\text{SiO}_2)$ increased in the range of 1.0:1–1.4:1, which demonstrated that 1250 °C was beneficial to the smelting process. Therefore, the smelting temperature of 1250 °C was adopted in the later experiments.

3.2 Effect of $m(\text{CaO})/m(\text{SiO}_2)$ on metal recovery rate and metal content in slag

The effect of $m(\text{CaO})/m(\text{SiO}_2)$ on metal recovery rate and metal content in slag was studied under the condition of 1250 °C for the smelting temperature, 60% for the oxygen concentration, 0.18 MPa for the gas pressure, 0.08 m³/h for the oxygen flow rate, 1 h for the reaction time, and 40 min for the clarification time.

Figure 6(a) shows the effect of $m(\text{CaO})/m(\text{SiO}_2)$ on metal recovery rate. According to Fig. 6(a), it was clear that the metal recovery rate increased as the $m(\text{CaO})/m(\text{SiO}_2)$ increased under the condition of $m(\text{Fe})/m(\text{SiO}_2)$ 1.1:1. The metal recovery rate increased from 56.17% to 88.30% when $m(\text{CaO})/m(\text{SiO}_2)$ increased in the range of 0.6:1–0.9:1. When CaO was added to the smelting system, the CaO molecules would dissociate into Ca^{2+} and O^{2-} with the increase of CaO content. Subsequently, the complex silicate ions in the slag

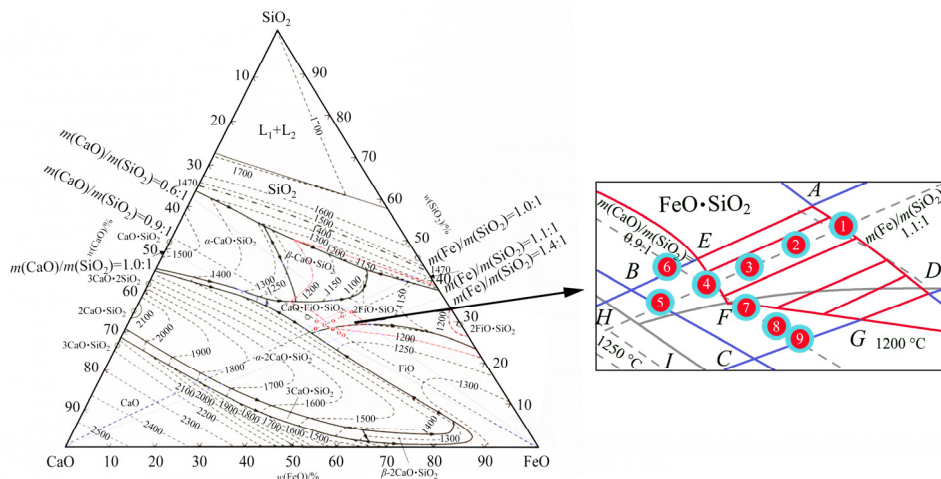


Fig. 4 Phase diagram of FeO–SiO₂–CaO ternary slag system [15]

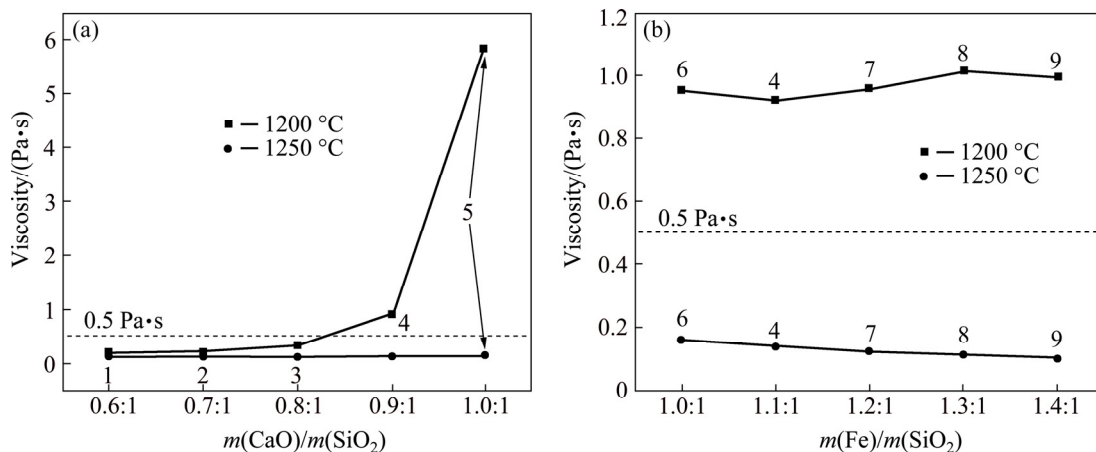


Fig. 5 Effect of $m(\text{CaO})/m(\text{SiO}_2)$ (a) and $m(\text{Fe})/m(\text{SiO}_2)$ (b) on viscosity of slag at different temperatures: (a) $m(\text{Fe})/m(\text{SiO}_2) = 1.1:1$; (b) $m(\text{CaO})/m(\text{SiO}_2) = 0.9:1$

would be dissociated into simple ions by means of $\text{Si}_2\text{O}_7^{6-} + \text{O}^{2-} \rightarrow 2\text{SiO}_4^{4-}$, $\text{Si}_4\text{O}_{11}^{6-} + 5\text{O}^{2-} \rightarrow 4\text{SiO}_4^{4-}$ and $\text{Si}_3\text{O}_9^{6-} + 3\text{O}^{2-} \rightarrow 3\text{SiO}_4^{4-}$, which would lead to the viscosity of slag to be reduced and the metal recovery rate to be augmented. However, the metal recovery rate decreased when $m(\text{CaO})/m(\text{SiO}_2)$ further increased to 1.0:1. This might be due to the dissociated SiO_4^{4-} ions would combine with Ca^{2+} to form Ca_2SiO_4 that would increase the viscosity of slag and diminish the metal recovery rate when the addition of CaO was too high [18,19].

Figure 6(b) presents the effect of $m(\text{CaO})/m(\text{SiO}_2)$ on metal content in slag. As shown in Fig. 6(b), the metal content in slag was below 1 wt.% when $m(\text{CaO})/m(\text{SiO}_2)$ increased in the range of 0.6:1–1.0:1. As discussed above, it can be seen that the metal recovery rate was the highest under the condition of $m(\text{CaO})/m(\text{SiO}_2)$ of 0.9:1, which belonged to a slag with high content of CaO. The slag with high content of CaO could enhance the surface tension of the slag, which was beneficial to

the accumulation settling of metal droplets [20,21]. Therefore, the slag with high content of CaO could effectively decrease the metal content in slag.

3.3 Effect of $m(\text{Fe})/m(\text{SiO}_2)$ on metal recovery rate and metal content in slag

The effect of $m(\text{Fe})/m(\text{SiO}_2)$ on metal recovery rate and metal content in slag was investigated under the condition of 1250 °C for the smelting temperature, 60% for the oxygen concentration, 0.18 MPa for the gas pressure, 0.08 m³/h for the oxygen flow rate, 1 h for the reaction time, and 40 min for the clarification time.

Figure 7(a) shows the effect of $m(\text{Fe})/m(\text{SiO}_2)$ on metal recovery rate. As shown in Fig. 7(a), it was discovered that the metal recovery rate increased first and then decreased as the $m(\text{Fe})/m(\text{SiO}_2)$ increased under the condition of $m(\text{CaO})/m(\text{SiO}_2)$ of 0.9:1. The metal recovery rate increased from 72.81% to 88.30% when $m(\text{Fe})/m(\text{SiO}_2)$ increased in the range of 1.0:1–1.1:1.

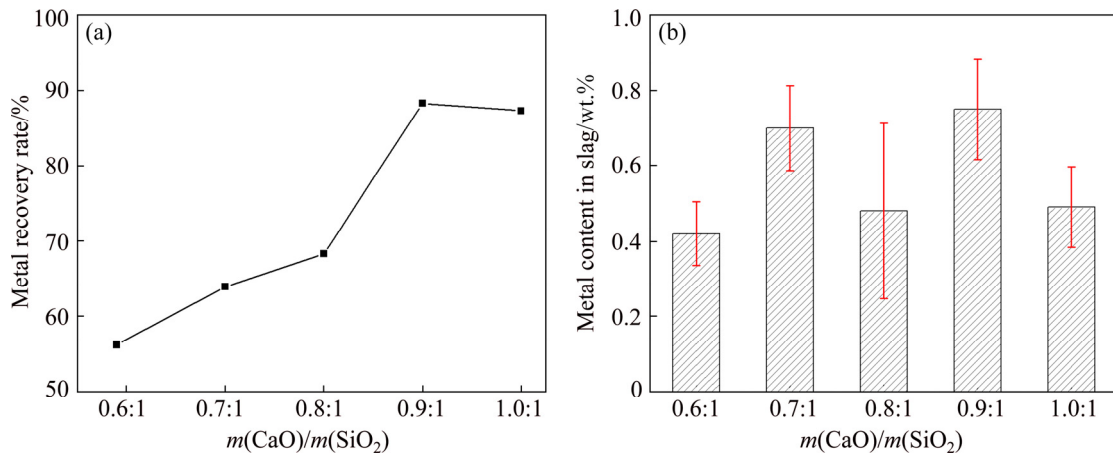


Fig. 6 Effect of $m(\text{CaO})/m(\text{SiO}_2)$ on metal recovery rate (a) and metal content in slag (b) at $m(\text{Fe})/m(\text{SiO}_2)$ of 1.1:1

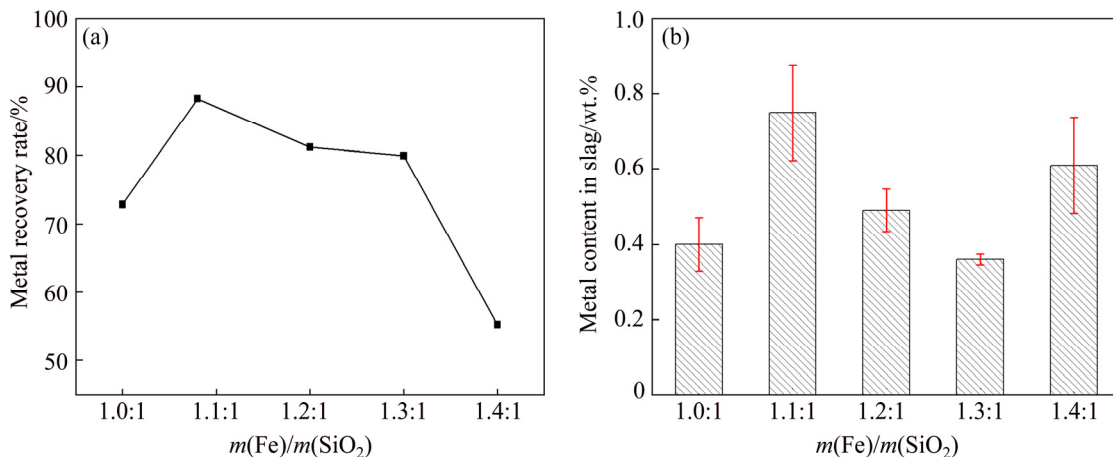


Fig. 7 Effect of $m(\text{Fe})/m(\text{SiO}_2)$ on metal recovery rate (a) and metal content in slag (b) at $m(\text{CaO})/m(\text{SiO}_2)$ of 0.9:1

When the Fe content in slag was low, the $\text{Si}_x\text{O}_y^{z-}$ ions in slag increased at low values of $m(\text{Fe})/m(\text{SiO}_2)$, which would increase the viscosity of slag, deteriorate the slag fluidity and diminish the metal recovery rate. With the increase of $m(\text{Fe})/m(\text{SiO}_2)$, the low melting compounds of kirschsteinite ($\text{CaO}\cdot\text{FeO}\cdot\text{SiO}_2$) and fayalite ($2\text{FeO}\cdot\text{SiO}_2$) could be formed during smelting, which would reduce the viscosity of slag and improve the metal recovery rate [22–24]. However, the metal recovery rate rapidly decreased from 88.30% to 55.28% when $m(\text{Fe})/m(\text{SiO}_2)$ further increased from 1.1:1 to 1.4:1. This might be because the high melting compound of calcium ferrite ($\text{CaO}\cdot\text{Fe}_2\text{O}_3$, melting point is 1420 °C) could be formed when $m(\text{Fe})/m(\text{SiO}_2)$ further increased, which sharply augmented the viscosity of slag and diminished the metal recovery rate [25].

Figure 7(b) shows the effect of $m(\text{Fe})/m(\text{SiO}_2)$ on metal content in slag. As presented in Fig. 7(b), the metal content in slag was below 1 wt.% when $m(\text{Fe})/m(\text{SiO}_2)$ increased in the range of 1.0:1–1.4:1. Therefore, $m(\text{Fe})/m(\text{SiO}_2)$ had little effect on the metal content in slag under the condition of $m(\text{CaO})/m(\text{SiO}_2)$ 0.9:1, which further illustrated that the slag with high content of CaO could effectively decrease the metal content in slag.

3.4 Microanalysis of smelting products

Figure 8 shows the XRD patterns of alloy and slag ($m(\text{Fe})/m(\text{SiO}_2)=1.1:1$, $m(\text{CaO})/m(\text{SiO}_2)=0.9:1$), indicating that the distinguishable crystal phase in the alloy mainly contained metallic lead, metallic antimony and a small amount of intermetallic compounds Cu_2Sb and FeSb_2 . The slag was mainly composed of kirschsteinite, fayalite, zinc oxide and zinc sulfide. The backscattered electron (BSE) images of alloy and slag (Fig. 9) further confirmed the observation from XRD. From the above analysis, it can be seen that the phases of Fe–Sb and Cu–Sb presented in the alloy had a negative effect on its quality, which further affected the metal recovery rate. Therefore, the recovery rate of the alloy could be improved by controlling the content of iron and copper in the alloy. Moreover, the lead and antimony phases were rarely found in the slag phase, which demonstrated that the slag with high content of CaO could effectively decrease the metal content in the slag.

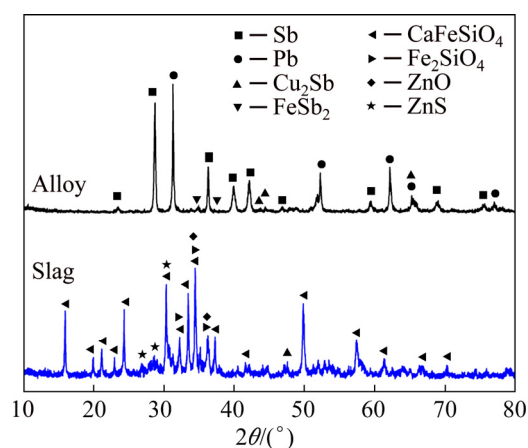


Fig. 8 XRD patterns of alloy and slag

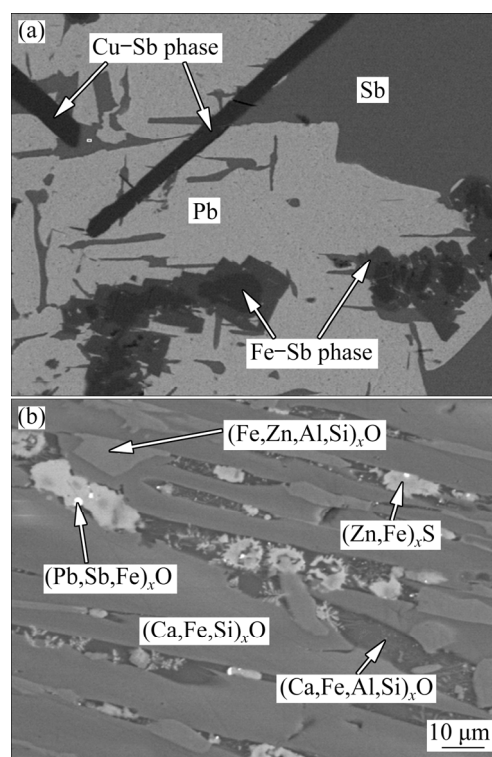


Fig. 9 Backscattered electron images of alloy (a) and slag (b)

4 Conclusions

(1) The viscosity of slag with $m(\text{Fe})/m(\text{SiO}_2)$ of 1.0:1–1.4:1, $m(\text{CaO})/m(\text{SiO}_2)$ of 0.6:1–1.0:1 was calculated by thermodynamic software Factsage. It was found that the viscosity of the slag was below 0.5 Pa·s at 1250 °C, which was beneficial to the smelting process.

(2) The experiment results indicated that the metal recovery rate of the smelting process could reach 88.30% and metal content (Pb+Sb) in the slag was lower than 1 wt.% under the condition of the

slag composition of 21–22 wt.% Fe, 19–20 wt.% SiO₂, 17–18 wt.% CaO with $m(\text{Fe})/m(\text{SiO}_2)$ of 1.1:1 and $m(\text{CaO})/m(\text{SiO}_2)$ of 0.9:1.

(3) The microstructure analysis of alloy and slag illustrated that the main phases in the alloy contained metallic lead, metallic antimony and a small amount of intermetallic compounds Cu₂Sb and FeSb₂. The slag was mainly composed of kirschsteinite and fayalite, and zinc in the raw material was mainly oxidized into the slag phase in the form of zinc oxide.

(4) Compared with earlier results which adopted the traditional routes for Pb–Sb alloy production from jamesonite concentrate, the oxygen-enriched direct smelting of jamesonite concentrate can improve the metal recovery rate. Moreover, the metal content in the slag was below 1 wt.%, indicating that the slag do not need to be further reduced in the blast furnace.

References

- [1] KRENEV V, DERGACHEVA N, FOMICHEV S. Antimony: Resources, application fields, and world market [J]. Theoretical Foundations of Chemical Engineering, 2015, 49(5): 769–772.
- [2] SUN Wei, SUN Chen, LIU Run-qing. Electrochemical behavior of galena and jamesonite flotation in high alkaline pulp [J]. Transactions of Nonferrous Metals Society of China, 2016, 26(2): 551–556.
- [3] ZHAO Cui-hua, CHEN Jian-hua, LI Yu-qiong. Electronic structure and flotation behavior of complex mineral jamesonite [J]. Transactions of Nonferrous Metals Society of China, 2015, 25(2): 590–596.
- [4] BARTLETT R W, MCCLINCY R J, WESELY R J. Smelting copper without converters [J]. JOM, 1985, 37(5): 17–19.
- [5] LI W F, ZHAN J, FAN Y Q. Research and industrial application of a process for direct reduction of molten high-lead smelting slag [J]. JOM, 2017, 69(4): 784–789.
- [6] GAN X P. Study of reasonable slag from Jinchuan's nickel flash smelting process [D]. Changsha: Central South University, 2002. (in Chinese)
- [7] FU Y M. Theoretical study and production practice of smelting slag in lead-blast furnace [J]. Rare Metals and Cemented Carbides, 1993(S1): 115–119. (in Chinese)
- [8] YANG B. Analysis on slag type selection of QSL lead smelting process [J]. China Nonferrous Metallurgy, 2004, 33(4): 27–28. (in Chinese)
- [9] ZHOU K J. Study on oxygen-enriched volatile bath smelting of stibnite concentrate and slag-type [D]. Changsha: Central South University, 2014. (in Chinese)
- [10] DAI X, CAI Y, LIAO C T, BIN W D, AN J G. A new process for oxygen-enriched direct smelting of jamesonite concentrate [C]//Proceedings of Forum of the China “12th Five-Year” Lead and Zinc Metallurgical Technology Development and Symposium of the Sixty Anniversary of Chihong Company. Qujing, 2010: 18–24. (in Chinese)
- [11] ZHANG Z T, DAI X, ZHANG W H. Thermodynamic analysis of oxygen-enriched direct smelting of jamesonite concentrate [J]. JOM, 2017, 69(12): 2671–2676.
- [12] CHEN M, DAI X. Microscopic study of the phase transformation during the oxygen-enriched direct smelting of jamesonite concentrate [J]. JOM 2018, 70(1): 41–46.
- [13] SATPATHY S, MISHRA S. Kinetics and mechanisms of solvent extraction and separation of La(III) and Ni(II) with DEHPA in petrofin [J]. Transactions of Nonferrous Metals Society of China, 2019, 29(7): 1538–1548.
- [14] ZHANG Bai-yong, PAN Xiao-lin, WANG Jiang-zhou. Reaction kinetics and mechanism of calcium oxide in dilute sodium aluminate solution with oxalate based on lime causticization [J]. Transactions of Nonferrous Metals Society of China, 2019, 29(6): 1312–1322.
- [15] LIU H Q, CUI Z X, CHEN M. Phase equilibria in the ZnO–“FeO”–SiO₂–CaO system at $P_{\text{O}_2} 10^{-8}$ atm [J]. Calphad, 2018, 61: 211–218.
- [16] LI L B. Study on the reduction of metal-rich slag of in oxygen-enriched direct smelting of jamesonite concentrate [D]. Changsha: Central South University, 2015. (in Chinese)
- [17] BALE C W, CHARTRAND P, DEGTEROV S A. FactSage thermochemical software and databases [J]. Calphad, 2009, 33(2): 295–311.
- [18] YAMNOVA N A, ZUBKOVA N V, EREMIN N N. Crystal structure of larnite β -Ca₂SiO₄ and specific features of polymorphic transitions in dicalcium orthosilicate [J]. Crystallography Reports, 2011, 56(2): 210–220.
- [19] PARK J H, JUNG I H, LEE H G. Dissolution behavior of Al₂O₃ and MgO inclusions in the CaO–Al₂O₃–SiO₂ slags: Formation of ring-like structure of MgAl₂O₄ and Ca₂SiO₄ around MgO inclusions [J]. ISIJ international, 2006, 46(11): 1626–1634.
- [20] WU Cheng-chuan, CHENG Guo-guang. Calculating models on surface tension of RE₂O₃–MgO–SiO₂ (RE=La, Nd, Sm, Gd and Y) melts [J]. Transactions of Nonferrous Metals Society of China, 2014, 24(11): 3696–3701.
- [21] HU Q S. Discussion on the effect of high ferrosilicon ratio on the treatment of gold concentrate and the effect of reducing lead in slag [J]. China Nonferrous Metallurgy, 1992(2): 36–41. (in Chinese)
- [22] QIAN G, SUN D D, TAY J H. Autoclave properties of kirschsteinite-based steel slag [J]. Cement and Concrete Research, 2002, 32(9): 1377–1382.
- [23] FOLCO L, MELLINI M. Crystal chemistry of meteoritic kirschsteinite [J]. European Journal of Mineralogy, 1997, 9(5): 969–974.
- [24] WILLIAMS Q, KNITTLE E, REICHLIN R. Structural and electronic properties of Fe₂SiO₄-fayalite at ultrahigh pressures: Amorphization and gap closure [J]. Journal of Geophysical Research: Solid Earth, 1990, 95(B13): 21549–21563.
- [25] DING C, LV X, CHEN Y. Crystallization kinetics of 2CaO·Fe₂O₃ and CaO·Fe₂O₃ in the CaO–Fe₂O₃ System [J]. ISIJ International, 2016, 56(7): 1157–1163.

Fe/SiO₂ 和 CaO/SiO₂ 质量比对脆硫铅锑精矿富氧直接熔炼过程合金直收率及渣中金属含量的影响

张忠堂, 戴曦

中南大学 冶金与环境学院, 长沙 410083

摘要: 通过改变渣相组成研究脆硫铅锑精矿在 1250 °C 时的富氧直接熔炼过程。探讨 Fe/SiO₂ 和 CaO/SiO₂ 的质量比对脆硫铅锑精矿富氧直接熔炼过程中合金直收率及渣中金属含量的影响。结果表明: 在 Fe/SiO₂ 质量比为 1.1:1、CaO/SiO₂ 质量比为 0.9:1、渣组成为(21–22)% Fe、(19–20)% SiO₂ 和(17–18)% CaO(质量分数)的条件下, 熔炼过程合金直收率达到 88.30%, 渣中金属(Pb+Sb)含量低于 1% (质量分数)。合金及炉渣工艺矿物学研究发现, 合金中主要物相为金属 Pb、金属 Sb 以及少量 Cu₂Sb、FeSb₂ 金属间化合物。炉渣主要由钙铁橄榄石和铁橄榄石组成, 原料中锌主要以氧化锌形式进入渣相。

关键词: 脆硫铅锑精矿; 冶金过程强化; 渣型; 火法冶金; 富氧直接熔炼

(Edited by Wei-ping CHEN)